

Artificial Intelligence in the Interpretation of Breast Cancer on MRI

Deepa Sheth, MD,* and Maryellen L. Giger, PhD

Advances in both imaging and computers have led to the rise in the potential use of artificial intelligence (AI) in various tasks in breast imaging, going beyond the current use in computer-aided detection to include diagnosis, prognosis, response to therapy, and risk assessment. The automated capabilities of AI offer the potential to enhance the diagnostic expertise of clinicians, including accurate demarcation of tumor volume, extraction of characteristic cancer phenotypes, translation of tumoral phenotype features to clinical genotype implications, and risk prediction. The combination of image-specific findings with the underlying genomic, pathologic, and clinical features is becoming of increasing value in breast cancer. The concurrent emergence of newer imaging techniques has provided radiologists with greater diagnostic tools and image datasets to analyze and interpret. Integrating an AI-based workflow within breast imaging enables the integration of multiple data streams into powerful multidisciplinary applications that may lead the path to personalized patient-specific medicine. In this article we describe the goals of AI in breast cancer imaging, in particular MRI, and review the literature as it relates to the current application, potential, and limitations in breast cancer.

Level of Evidence: 3

Technical Efficacy: Stage 3

J. MAGN. RESON. IMAGING 2020;51:1310–1324.

BREAST CANCER is the second leading cause of death among women in the United States. Over 40,000 women were estimated to die of breast cancer in 2016.¹ Early detection is key to improved survival, and the overall prognosis is directly linked to the stage of disease at the time of diagnosis.² Screening with mammography is associated with a 16–40% relative reduction in breast cancer mortality among women aged 40–74 years old.^{3,4} However, cancers can be missed at mammography, particularly in women with dense breasts.⁵ Screening with mammography alone may be insufficient in the screening of women who are at high risk of breast cancer.⁶ The need for more effective screening strategies to supplement mammography in these groups of women has led to the emergence of newer imaging techniques for supplemental screening, including dynamic contrast-enhanced (DCE) breast magnetic resonance imaging (MRI), digital breast tomosynthesis (DBT), and automated whole breast ultrasound (AWBUS).

The expanding and diversifying role of newer imaging techniques in breast cancer has provided radiologists with increasing datasets and varied multimodality diagnostic tools,

all of which are differentially applied in various clinical scenarios. Artificial intelligence (AI) offers the opportunity to streamline and integrate the diagnostic expertise of the radiologist, including the recognition and stratification of complex patterns in images, clinical translation of tumoral phenotype to genotype, and outcome prediction as it relates to therapeutic and prognostic plans.

AI-aided systems, such as Computer-Aided Detection (CADe) and Computer-Aided Diagnosis (CADx), have been under development and/or in clinical use for decades, aiding radiologists in converting image data to quantitative data.^{35,47} Radiomics, an expansion of CADx, has been defined as the conversion of images to mivable data.¹¹ Radiomic data may involve computer segmentation of a tumor from its background parenchyma followed by extraction of various tumor features. The extraction of large volumes of quantitative data from radiologic images, combined with patient-specific clinical data, lends itself to radiogenomics, the combination of radiomic data with genomics and other "-omics" data.⁶⁷ Incorporating radiogenomics with breast imaging has the potential to 1) correlate image-specific phenotypes with

View this article online at wileyonlinelibrary.com. DOI: 10.1002/jmri.26878

Received Apr 30, 2019, Accepted for publication Jul 8, 2019.

*Address reprint requests to: D.S., Department of Radiology, University of Chicago, 5841 S Maryland Ave., Rm. P221, MC 2026, Chicago, IL 60637.
E-mail: dsheth@radiologybsd.uchicago.edu

From the Department of Radiology, University of Chicago, Chicago, Illinois, USA

underlying genetic mutations, tumor profiles, and hormonal receptor status; 2) develop imaging biomarkers that incorporate tumor- and patient-inherent characteristics to predict outcomes and prognosis; and 3) begin to risk-stratify patients with personalized imaging guidelines leading the way to precision medicine.

It is also of interest to explore AI in breast cancer imaging in terms of deep-learning-based methods. Learning directly from the image data has led to deep-learning methods for content-based retrieval, CAD, and data mining.^{47,48} Ultimately, merging conventional radiomics with deep learning could lead to advanced predictors.⁵⁶

Different approaches to extract information from medical images are available that require varying degrees of input from a radiologist to identify or characterize the region of interest. The features of interest can be extracted either through human input, semiautomatic process, or fully automatic processes. Human feature extraction has the advantage of being readily evaluated without sophisticated post-processing or software. However, it has substantial inter- and intraobserver variability, resulting in weaker radiogenomic correlations, and often times it is time-consuming, limiting application in real clinical practice. Due to these drawbacks, semi- and fully automatic approaches for image feature extraction are preferred.³⁵ Hand-crafted (aka human-engineered) features include various characteristics of the breast lesion and parenchyma including tumor size, shape, margin sharpness, and texture, as well as kinetics (if applicable).^{9,35} Deep-learning methods indirectly characterize by inputting the image data directly into the deep-learning network (such as a convolutional neural network, CNN) (Fig. 1).

The traditional approach of "one-size-fits-all" represents a philosophy of universal imaging and treatment guidelines for the patient. In contrast, precision medicine represents a philosophy of focused strategies for specific groups of individuals, according to their (and their disease's) genetic, phenotypic, and environmental characteristics. The combination of image-specific findings with the underlying genomic, pathologic, and clinical features is becoming of increasing value in breast cancer. The concurrent emergence of newer imaging techniques has provided radiologists with greater diagnostic tools and image datasets to analyze and interpret. Integrating an AI-based workflow within breast imaging enables the integration of multiple data streams into powerful multidisciplinary systems that may lead the path to personalized patient-specific medicine.

In this article we describe the goals of AI in breast cancer imaging, in particular MRI, and review the literature as it relates to the current application, potential, and limitations in breast cancer. The organization of the article follows the clinical usage of breast imaging in the detection, workup, and patient management. Detection usually occurs at the screening of asymptomatic patients, requiring computers to conduct a localization task, while diagnosis occurs at the workup of symptomatic patients, requiring computers to perform diagnostic and prognostic tasks.

Detection

Detection refers to the localization of objects of interest in images, used in Computer-Aided Detection (CADe).^{8,9} The detection of cancer by radiologists is limited by multiple factors, including the presence of structural noise (ie, dense breast parenchyma obscuring an underlying malignant lesion), incomplete visual search patterns, incorrect assessment of subtle or complex

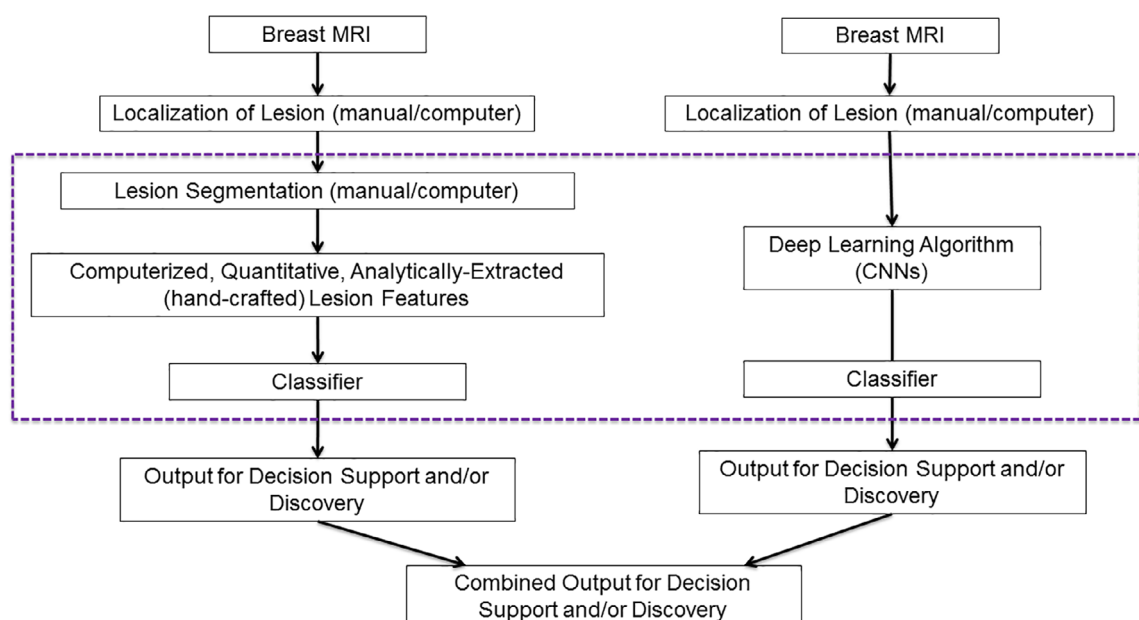


FIGURE 1: Schematic illustrating both (left) analytical radiomic-based (human-engineered) CAD and (right) deep-learning-based CAD along with a means to combine output for improved performance.

disease states, vast amounts of image data, suboptimal physical image quality, fatigue, and distractions. Integration with AI-based detection tools can be used as a localization task and serve as a companion to radiologists in their task of finding suspicious lesions within images.

Computer image enhancement systems were developed to aid radiologists in interpreting breast MRI, especially DCE-MRI. These systems have the potential to reduce reading time and reduce diagnostic errors since they are able to highlight lesions of suspicion, including those that might be misinterpreted or overlooked by radiologists during breast MRI screening.¹² Most breast MR image analysis algorithms rely on the full-breast MRI protocol, including the temporal information from the late-phase scans and the morphological information from the early-phase scans. Investigators have reported on CADe systems, which indicate locations of potential suspicious lesions on DCE-MRIs based on morphology and kinetics.^{68,69}

Of the available modalities for evaluation of the breast, MRI has been found to have the highest sensitivity for the detection of breast cancer, irrespective of breast density.¹⁴ On the basis of evidence from nonrandomized trials and observational studies, breast MRI is currently indicated as a supplement to mammography for patients at high risk, with greater than 20% relative lifetime risk.¹⁵ However, for women at intermediate risk, including those with dense breast tissue,

screening MRI in the United States is still growing. One way to achieve the efficiency and rapid throughput found with screening mammography is to shorten screening breast MRI protocols, decrease image acquisition time, and shorten image interpretation time. Use of abbreviated and ultrafast MRI protocols could result in lower cost and faster throughput, increasing availability and providing women with dense breasts or at intermediate risk (lifetime risk, 15–20%) greater access to breast MRI.¹⁶ However, these rapid advances in MRI acquisition technique come at the sacrifice of delayed phase kinetic data (Fig. 2).

The initial development of computer detection systems for breast abnormalities was conducted on digitized mammograms, followed later on by FFDM (full-field digital mammograms), and these have been extensively reviewed over the decades.^{9,35} Human-engineered methods were initially used in the detection of masses and clustered microcalcifications in which computers processed the mammograms to enhance the signals of the lesions followed by computer extraction (feature extraction) of lesions and false-positive detections. Interestingly, the implementation of deep networks for lesion detection in breast imaging was also conducted on mammography for use in screening programs, with the first such instance in 1994 in which a shift-invariant (aka CNN) was used in the detection of microcalcifications^{49–51} (Fig. 3). Translation of such computer-aided detection systems later occurred with evaluations on multiinstitutional cases.⁸⁰ Over the past decades, AI advances on breast imaging for detection mainly resided with the breast imaging modalities used in screening, ie, FFDM and tomosynthesis.

Now, however, as the role and protocol variations of MRI increase for use as an adjunct to mammographic screening, additional AI detection techniques for breast MRI are being developed. Dalmis et al are developing a CADe system using deep learning that relies on early-phase spatial information as opposed to late-phase temporal information. Their CADe system performed significantly higher than their previous CADe system, demonstrating possible usage in abbreviated MRI protocols.⁴⁶ Future CADe systems that can extract information from early-phase scans will be of increasing value to radiologists.

It is interesting to note that for computer-aided detection, the benefit to the radiologist may be contributed through effectiveness and/or efficiency, depending on the complexity of the imaging exam. Multiparametric MRI lends itself to computer analysis given the image-integration required by the human eye-brain system during the detection process.

Diagnosis

Diagnosis typically refers to the workup of a breast lesion once it is detected by either imaging or other means, such as physical exam. Thus, it is not a localization task but rather a classification task, and at this clinical step, multiple breast modalities are

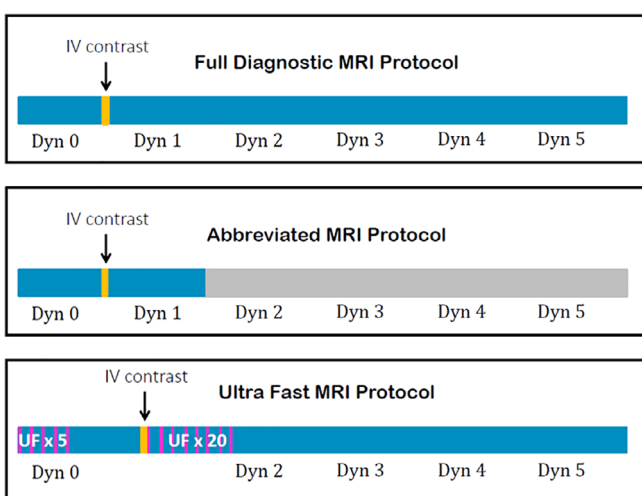


FIGURE 2: Schematic depicting three different MRI protocols including a full DCE diagnostic MRI, an abbreviated MRI, and an ultrafast MRI. The full diagnostic MRI is the default protocol used in all clinical settings with the acquisition of one precontrast and multiple postcontrast sequences. The abbreviated MRI protocol involves the acquisition of a single precontrast and single postcontrast sequence. The ultrafast MRI protocol involves the acquisition of several high temporal resolution (temporal resolution of 3–7 sec) sequences during the pre- and postcontrast phase. All three of these protocols vary in exam duration, sequence acquisition, and temporal resolution, allowing radiologists to use different protocols for different purposes. Additional sequences, including T₂-weighted and DWI, are not included in this schematic.

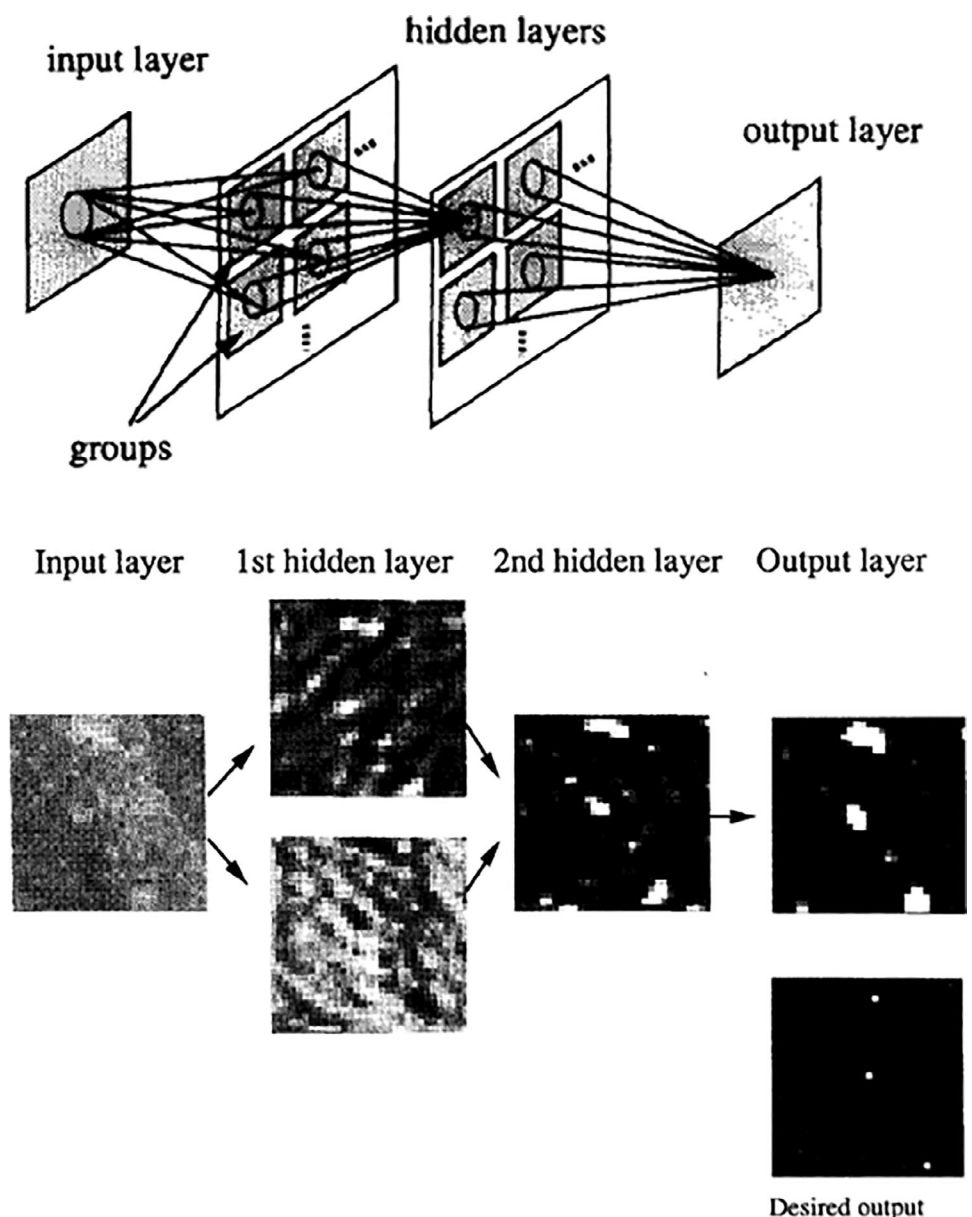


FIGURE 3: Illustration of the first publication of a CNN (aka shift-invariant neural network) used in medical image analysis. The network was used in the computer detection of microcalcifications on digital mammograms. Reprinted with permission from Medical Physics (Ref. 51).

often used, requiring integration of findings. Diagnosis refers to the segmentation, characterization, and staging of tumors, collectively known as Computer-Aided Diagnosis (CADx). CADx involves the automatic characterization of a region or tumor, initially indicated by either a radiologist or a computer, after which the computer characterizes the lesion of interest and estimates a likelihood of malignancy, leaving the workup or therapeutic management plan to the clinicians⁹ (Fig. 4). Note that most such systems are developed and trained using biopsy results as the pathological "truth."

For many years, clinical image analysis systems, which are used during interpretation of MRIs for diagnostic workup, have included software applications that indicate

areas of enhancement along with their voxel-by-voxel kinetic curves and corresponding threshold levels.⁷² However, with CADx the goal is to output lesion characteristics (ie, radiomic features) as well as a tumor signature that is related to the likelihood that the lesion in question is a cancerous tumor. Over the decades, Giger and colleagues have developed and clinically translated such a system, which includes automatic lesion segmentation, feature extraction, and the merging of features into a tumor signature, and have demonstrated improvement in radiologist performance in the task of classifying between malignant and benign tumors^{52–55,81} (Fig. 5a, b). These human-engineered radiomic approaches were later augmented with deep-learning approaches.^{56,57}

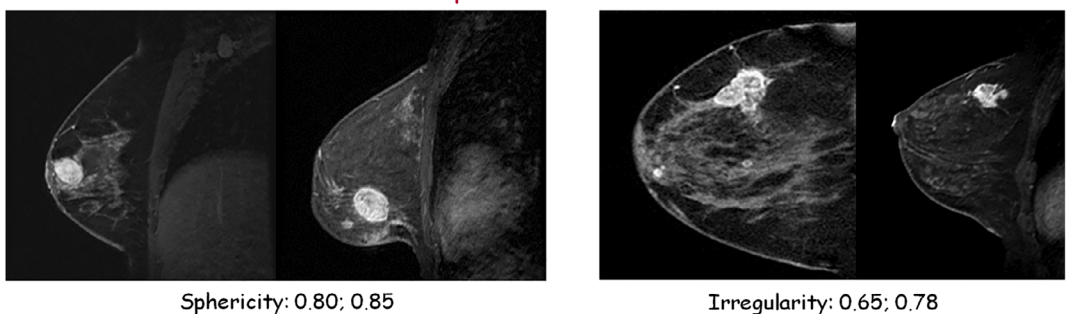
Shape of Breast Tumors

FIGURE 4: Computer machine-learning algorithms continue to be developed to facilitate tumor diagnosis, segmentation, and feature extraction on MRI. In contrast to the qualitative nature of human extracted imaging phenotypes, the quantitative characteristics of computer extracted imaging phenotypes (CEIP) may improve the reproducibility, accuracy, and predictive power of breast imaging. CEIP may be able to identify specific imaging features that could become biomarkers for tumor biology, predictors of treatment response and surrogates for genetic testing. Reprinted with permission from M.L. Giger, University of Chicago.

Such CADx systems vary in the tumor extraction, with some using semiautomated and others incorporating automated lesion segmentation methods. Song et al have incorporated the processing of quantitative tumor features, allowing for more reproducible descriptors particularly as they relate to tumor volume, extent, and multifocality.¹⁰ Meinel et al created a breast MRI CAD system that improved the performance of all interpreting readers in classifying lesions. The CAD system was based on a backpropagation neural network that was trained on 80 breast MRI lesions that were manually segmented by an expert radiologist. Of note was the decrease in false-positives and follow-up imaging as a result of implementation of the CAD system.⁷⁸ Dalmis et al developed a CADx system for high spatiotemporal resolution DCE-MR images using radiomic features.¹³ Characterizing the most enhancing regions within the lesion has been shown to be beneficial in assessing the likelihood of malignancy. Chen et al developed a method to identify the most enhancing voxels within a tumor using unsupervised fuzzy c-means clustering, which was further validated by Chang et al.^{53,70}

Similar to the application of AI methods to breast imaging data, radiomic characteristics extracted from DCE-MRI can be correlated with various tumor-specific features. Lesion characterization methods analyzing the kinetics of uptake in DCE-MRI have been investigated for the interpretation of clinical breast images. Platel et al performed lesion characterization using ultrafast high temporal resolution DCE-MRI and found that the classification performance was significantly higher with kinetics derived from ultrafast DCE-MRI than that from regular DCE-MRI.²² Wu et al examined the relationship between automatically computed quantitative contrast enhancement kinetics of normal breast parenchyma and the presence of breast cancer, demonstrating an association between features related to signal enhancement independent of mammographic density and background parenchymal enhancement.²³

Deep learning through convolutional neural networks has now been applied to the characterization task in the diagnostic workup of breast tumors in mammography/tomosynthesis, ultrasound, and MRI.⁵⁶⁻⁶¹ In the task of distinguishing between malignant and benign breast lesions, transfer learning has been used with a pretrained CNN either through feature extraction or fine tuning. When using deep learning in classification, the image data of the tumor within a region of background, as opposed to the full image, are input to the CNN in order to avoid having distal nontumor-related image regions interfering with the deep-learning method.

Due to limited datasets, investigators have looked at the benefit of using various forms of processed image data as input to the CNN. For example, Antropova et al found with DCE-MRI that using MIP (maximum intensity projection) images instead of early-phase unsubtracted or subtraction images yielded improved deep-learning computer performance⁵⁷ (Fig. 6).

As advances in human-engineered radiomics and deep learning grow, combinations of both need to be continuously investigated in order to optimize the benefits that each bring to the classification task.^{56,62,82,83} While the most recent published studies involve more than 500 cases, databases are growing as investigators realize that both the number and distribution of cancers and noncancers are crucial to the development and validation of CADx systems.

Prior studies have reported significant correlations between MRI enhancement kinetics and molecular breast cancer subtypes.²¹ In a multiinstitutional National Cancer Institute research study, the relationships between computer-extracted radiomic MRI features and various clinical, molecular, and genomic markers were investigated.^{18,67} Statistically significant associations were seen between the enhancement texture radiomic features and molecular subtypes (such as luminal A, luminal B, HER2-enriched, basal-like). Wu et al studied the relationship between tumor and background parenchymal enhancement with breast cancer molecular

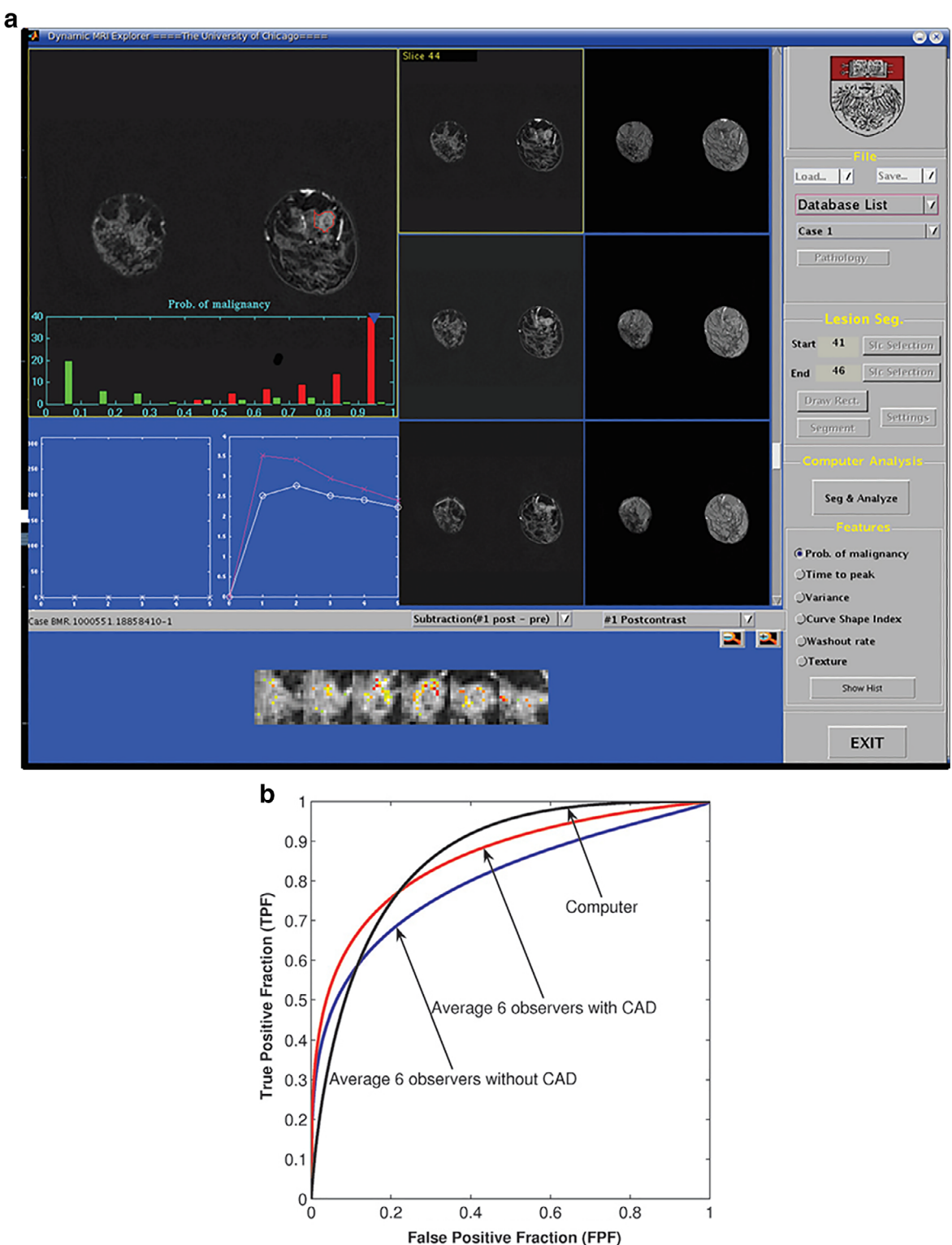


FIGURE 5: (a) User interface in the testing of CADx in a reader study. MR images and computer-extracted information are displayed including segmented lesions (outlined in red); an estimated probability of malignancy relative to a training database of approximately half cancers; a histogram plot showing distributions of malignant (red) and benign (green) lesions with a blue arrowhead indicating case in question; two kinetic curves with lower (white) curve indicating average lesion signal intensity over time and upper (pink) curve indicating computer-identified most-enhancing signal intensity over time; and images showing the most-enhancing regions within the given lesion. (b) ROC curves showing performances of all six readers without and with CADx as well as the computer alone. The six readers demonstrated a statistically significant improvement in performance in distinguishing between malignant and benign lesions. The mean AUC increased from 0.80–0.84 with CADx ($P = 0.007$). Reprinted with permission from Radiology (Ref. 55).

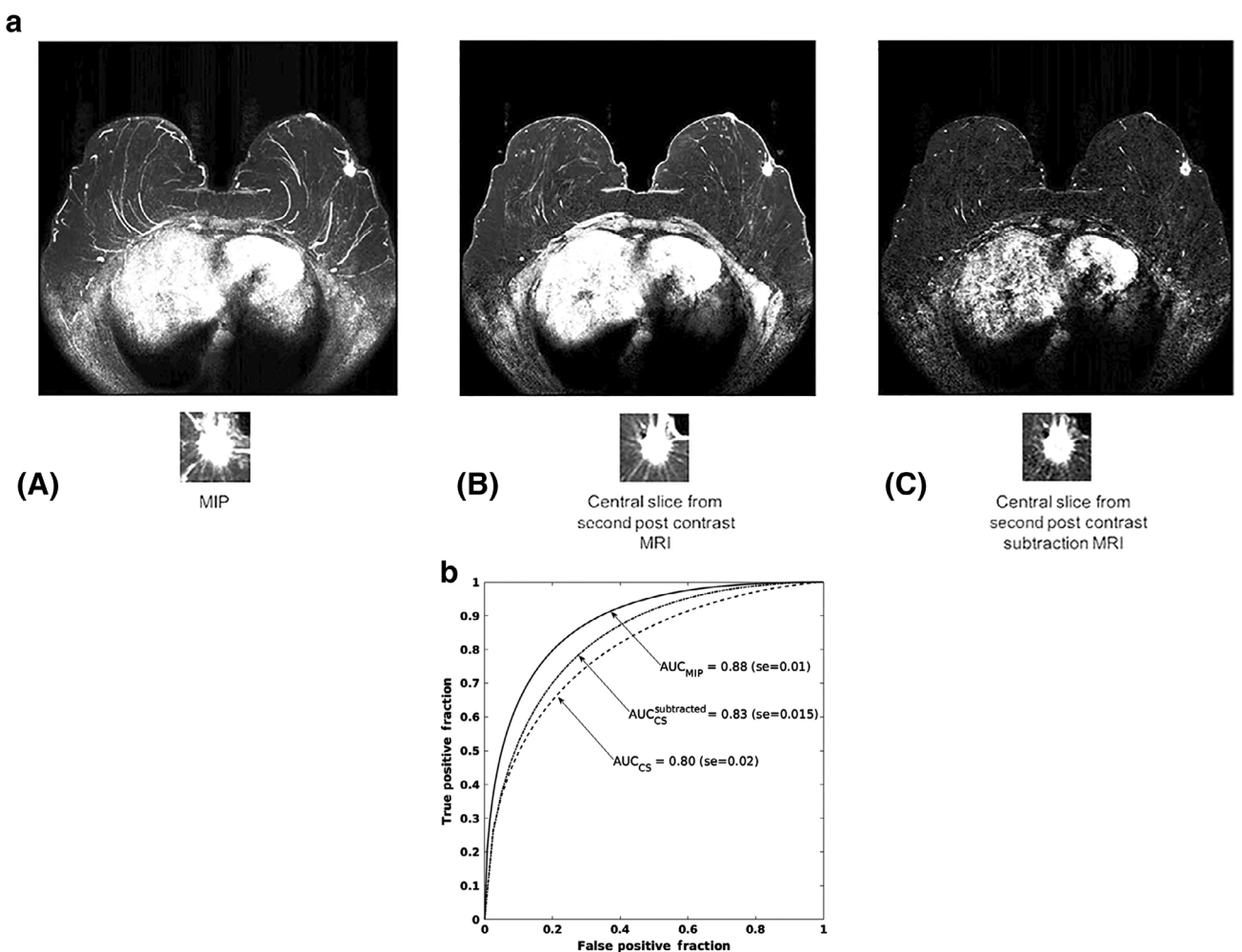


FIGURE 6: Example of a malignant lesion imaged by MRI (a) the MIP image of the second postcontrast subtraction MRI, (b) the center slice of the second postcontrast MRI, and (c) the central slice. ROC curves showing the performance of three classifiers. Classifiers were trained on CNN features extracted from regions of interest selected on: (a) the MIP images of second postcontrast subtraction MRIs, AUC_{MIP} , (b) the central slices of the second postcontrast MRIs, AUC_{CS} , and (c) the central slices of second postcontrast subtraction MRIs, $AUC_{Subtracted\ CS}$. Reprinted with permission from Journal of Medical Imaging (Ref. 57).

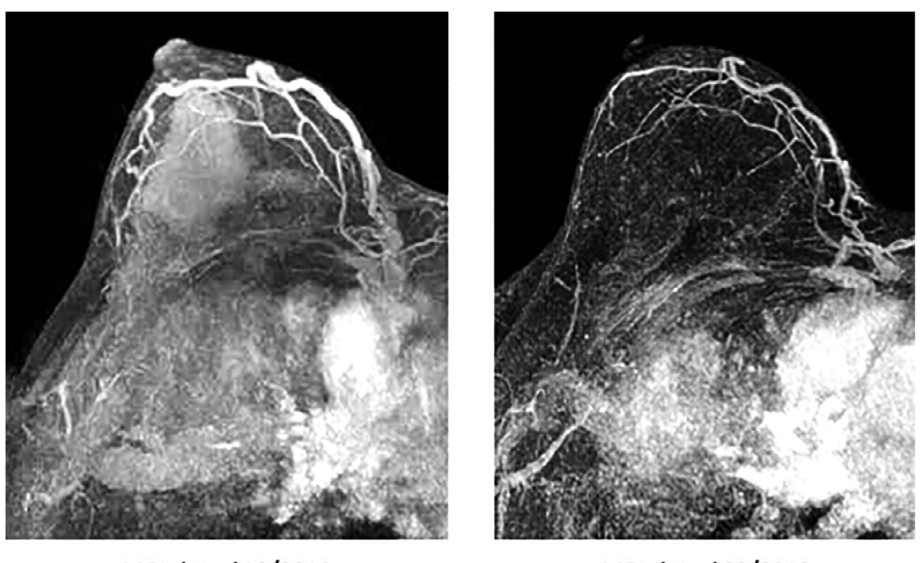


FIGURE 7: DCE MR maximum intensity projection images of the same patient undergoing neoadjuvant therapy for biopsy-proven malignancy of the right breast. The two images are separated by 4 months, during which time the patient had a complete imaging response on repeat MRI.

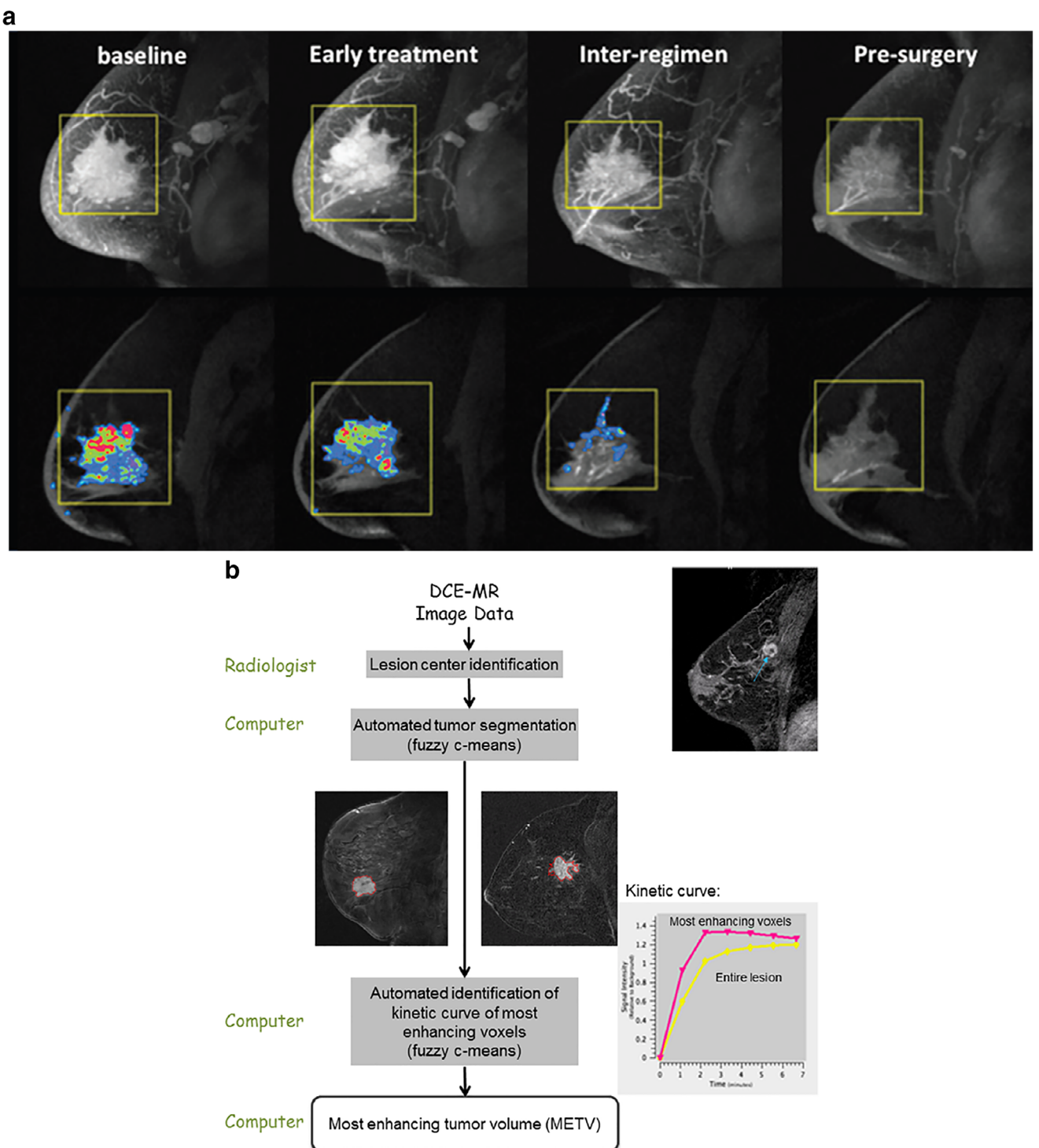


FIGURE 8: (a) Serial maximum intensity projection images with corresponding functional tumor volume (FTV) maps. Semiautomated computer analysis of contrast-enhanced images were used to compute the FTV by using the signal enhancement ratio method. Reprinted with permission from Radiology (Ref. 30). **(b)** On a dataset of breast cancer cases, the most-enhancing tumor volume (METV), which was automatically determined from the most-enhancing regions within a DCE-MRI tumor, was found to be predictive of recurrence-free survival. This method involved the manual indication of the approximate tumor center with subsequent real-time automatic lesion segmentation and feature extraction, yielding a promising practical tool for clinical application. Reprinted with permission from Cancer Imaging (Ref. 64).

subtypes, with area under the curve (AUC) values between 0.66 and 0.79 obtained in distinguishing different molecular subtypes of breast cancer.¹⁸ Grimm et al included 278 breast cancer patients and found significant correlations between

molecular subtypes and DCE-MRI Breast Imaging-Reporting and Data System (BIRADS) features.¹⁹ They found statistically significant associations between Luminal A and Luminal B cancers with MRI radiomic features. Li et al used data from

the TCGA to demonstrate associations between radiomic MRI tumor features and molecular subtypes.⁶³

Treatment Response and Risk of Recurrence

The use of neoadjuvant systemic therapy in the treatment of breast cancer patients is increasing beyond the scope of locally advanced disease.⁷¹ The role of imaging to assess response to therapy is expanding into translatable and clinically relevant therapeutic and prognostic recommendations. Current methods for evaluating tumor response to neoadjuvant therapy consists of physical examination and conventional breast imaging with mammography, ultrasound, and/or MRI.

Breast MRI is the most sensitive modality for breast cancer detection and is the most accurate for assessment of tumor response to neoadjuvant therapy²⁴⁻²⁷ (Fig. 7). A prospective, multiinstitutional trial that validated the accuracy of breast MRI for assessment of response to neoadjuvant therapy was the American College of Radiology Imaging Network (ACRIN) 6657 study, which was performed in conjunction with the multiinstitutional Investigation of Serial Studies to Predict Your Therapeutic Response with Imaging And molecular Analysis (I-SPY TRIAL).²⁹ The highest predictive value for predicting pathologic response after neoadjuvant chemotherapy was

achieved by using both MRI and clinical measurements of tumor size.²⁹ Using a CNN to predict pathologic complete response from the ISPY database, Ravichandran et al were able to produce probability heatmaps that demonstrated tumor regions most strongly associated with therapeutic response. The addition of various clinical prognostic variables (including age, largest diameter, and hormonal status) further increased the association.⁷⁹ As shown by Drukker et al, the use of radiomics with automated tumor segmentation yielded an automatic method for computing the computer-extracted most-enhancing tumor volume (METV) with similar performances in predicting recurrence-free survival but without the manual aspects.⁶⁴ The automated capabilities of AI offer the potential for effective and efficient volumetric demarcation of tumor size serially over time and accurate tracking of multiple lesions in a quantifiable and repeatable manner (Fig. 8a,b).

Another application of radiogenomics is the correlation of MRI features of breast cancer with clinically available genomic assays, which provide prognostic scores representing risk of cancer recurrence and thus can be helpful for guiding treatment decisions. The 21-gene Oncotype DX assay, the 50-gene PAM50 assay, and the 70-gene MammaPrint microarray assay are multi-gene assays that correlate breast cancer expression profiles to risks of cancer recurrence.³¹⁻³³ The qualitative data extracted from

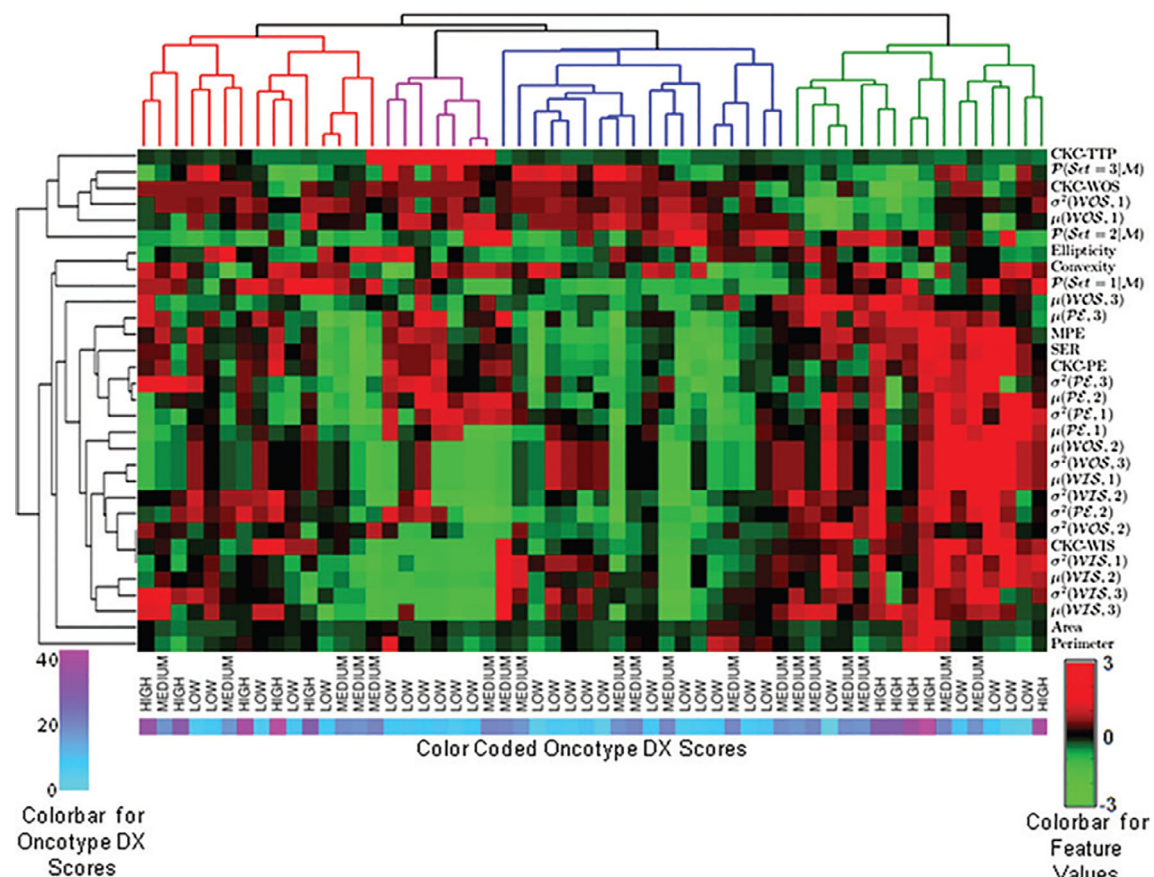


FIGURE 9: Color heatmap with columns representing tumors and rows representing DCE MRI features. Unsupervised hierarchical clustering identified specific intrinsic imaging phenotypes for breast cancer that were associated with specific prognostic gene expression profiles. Reprinted with permission from Radiology (Ref. 20).

MRI might be a potential imaging biomarker for breast cancer risk recurrence. Ashraf et al²⁰ investigated the relationship between computer-extracted MRI features of tumor structure, function, and heterogeneity and gene expression using OncotypeDx. Four features (related to tumor enhancement pattern and tumor size) correlated with recurrence score, demonstrating that tumors with greater neoangiogenesis were associated with an increased risk of recurrence²⁰ (Fig. 9). Li et al further investigated this concept by using computer-extracted breast MRI phenotypes to predict the risk of breast cancer recurrence using clinically available multigene assays, demonstrating that tumors with a high risk of recurrence were shown to be larger, with more heterogeneous enhancement.²¹ Correlating computer-extracted imaging data from DCE MRI with inherent tumoral features shows early promise, particularly with regards to refining tumor categorization and predicting risk recurrence. Continued development in radiomic MRI features with or without deep learning may allow for precise imaging signatures that can direct diagnostic and therapeutic plans specific to the individual patient.

Personalized approaches to individual tumors may lead to earlier initiation of therapeutic plans, deeper understanding of tumor prognostics, and improved patient outcomes. Such was the goal of the multiinstitutional National Cancer Institute in mapping computer-extracted radiomic MRI features to genomic markers⁶⁷ (Fig. 10).

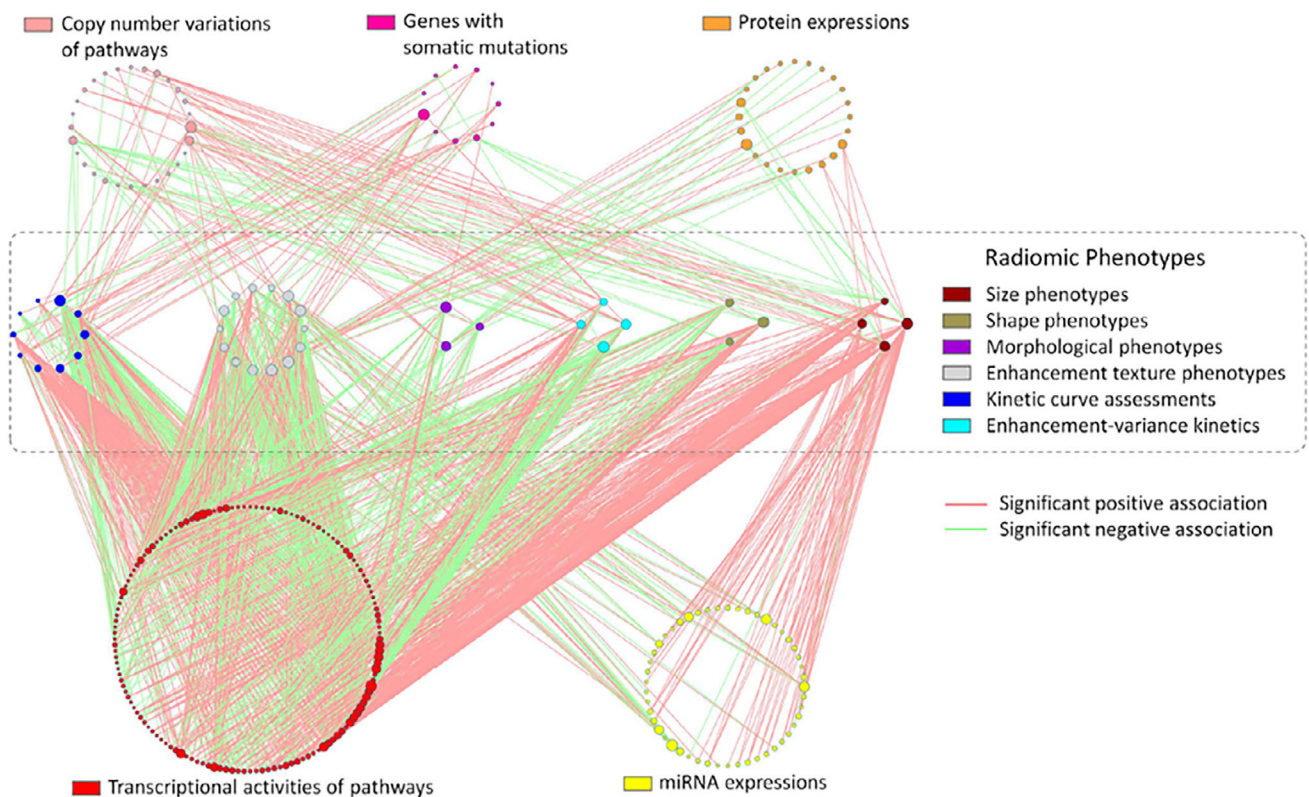


FIGURE 10: Significant associations between genomic features and radiomic phenotypes in breast cancer as identified by DCE MRI. Each line is an identified statistically significant association, whereas nonsignificant associations are not depicted. Node size is proportional to its connectivity relative to other nodes in the category. Reprinted with permission from Nature Scientific Reports (Ref. 67).

Risk Assessment and Prevention

Risk assessment tools allow for the estimation of a women's lifetime risk of breast cancer. Accurate assessment of risk allows for the application of risk-stratified screening regimens and preventive therapies to reduce overall risk. The various breast cancer models incorporate different risk factors in the calculation, including demographics, personal history, family history, hormonal status, and hormonal therapy. Emerging evidence suggests that incorporation of breast density may further stratify patients.⁷⁶

Breast density and parenchymal patterns of breast density have been shown to have a role in estimating breast cancer risk.³⁶ Breast density describes the relative amount of fibroglandular tissue to adipose tissue in the breast. The risk of breast cancer increases steadily with increasing mammographic breast density.³⁹ This direct association is felt to be due to two effects: the masking effect and the biologic effect. The masking effect describes the influence of superimposing dense fibroglandular tissue on the interpreting radiologists' ability to detect lesions, leading to an overall decrease in mammographic sensitivity with increasing breast density. The biologic effect describes the inherently increased risk of breast density as an independent risk factor, felt to be due to a number of associations including hormonal and growth factors.⁷³

The risk of breast cancer in women with mammographically dense breasts is three to five times higher than that in women with predominantly mammographically nondense (fatty)

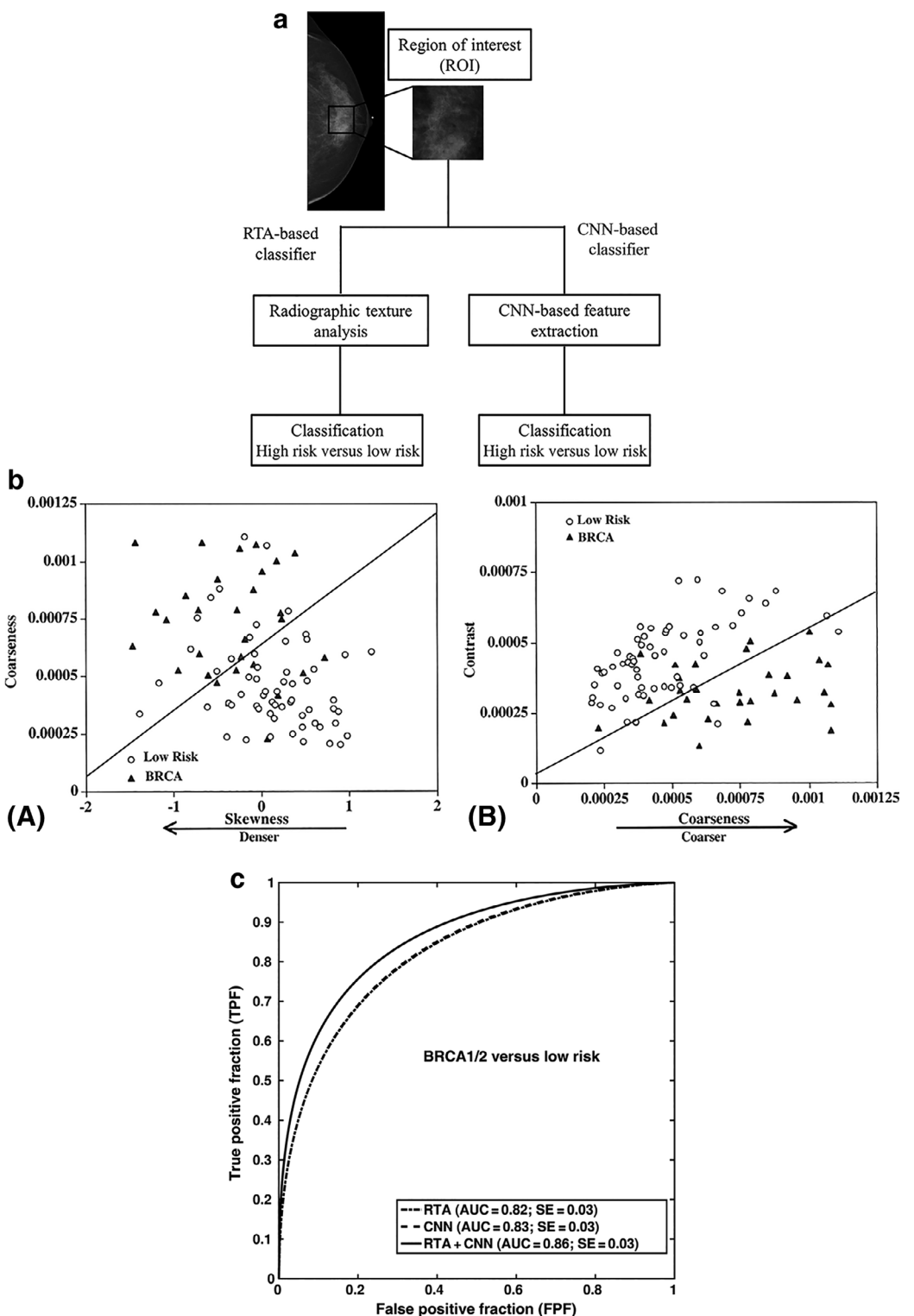


FIGURE 11: (a) Schematic diagram of radiomic texture analysis (RTA) and deep CNN-based methods for breast cancer risk assessment (Ref. 62). (b) Scatterplots show distributions of 60 low-risk cases and 30 *BRCA1* and *BRCA2* mutation carriers in an age-matched group in terms of radiomic features of (a) skewness vs. coarseness and (b) coarseness vs. contrast. As indicated by the separation line, the mutation carriers tended to have more dense breast tissue, with coarser and lower contrast texture patterns on their mammograms, than did the low-risk women in the age-matched group (Ref. 37). (c) ROC curves indicating the performance of RTA-based, CNN-based, and fusion classifiers in the task of distinguishing between *BRCA1/2* gene-mutation carriers and low-risk women (Ref. 62). Reprinted with permission from Journal of Medical Imaging (a,c) and Radiology (b).

breasts.⁴² Early studies with *BRCA1* and *BRCA2* carriers have shown that computerized measures of mammographic parenchymal texture (aka radiomic texture) from the retroareolar breast

region can distinguish *BRCA1/2* carriers from low-risk women.³⁷ Recent studies of screening populations have shown that features of parenchymal texture extracted from screening mammograms

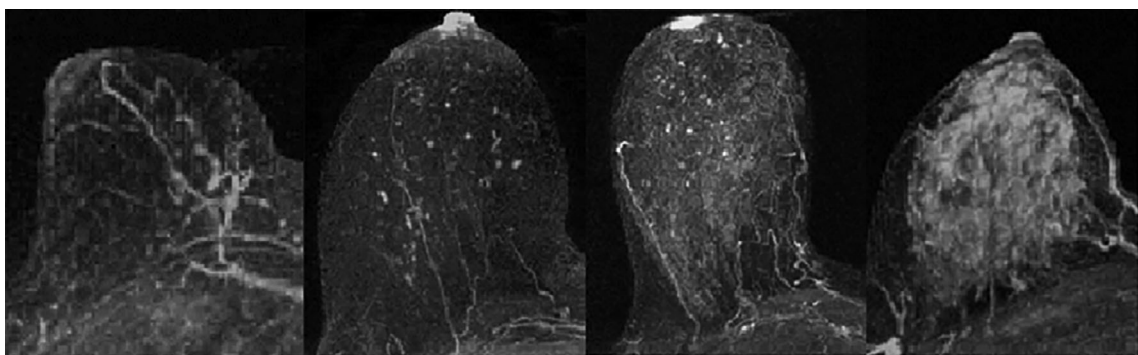


FIGURE 12: Schematic depicting the four categories of breast parenchymal enhancement (BPE) as defined by the enhancement of the fibroglandular tissue of the breast(s) after the intravenous administration of contrast material. The four categories include (listed from low to high levels of enhancement): minimal, mild, moderate, and marked. Reprinted with permission from Constance Lehman, University of Washington.

(either from the retroareolar region or the entire breast area) are significantly associated with breast cancer independent of breast density.³⁸ This association with breast cancer risk suggests a possible mechanism of correlating underlying biological processes with resultant imaging phenotypes. Deep learning is also being examined for use in assessing breast density and in describing the parenchymal patterns of density on mammograms^{65,66} (Fig. 11a–c).

Similar to breast density in mammography, the amount of fibroglandular tissue (FGT) seen on MR images and the level of background parenchymal enhancement (BPE) after contrast administration are features of normal breast tissue. The amount of FGT to the breast volume determines the breast density. Dalmis et al used a deep-learning method called U-net to accurately quantify breast density.⁷⁴ This deep-learning method outperformed existing methods and was able to overcome variations in MRI protocols, breast shapes, and breast volumes. The level of BPE refers to the volume and intensity of the enhancement of normal breast tissue after the administration of intravenous contrast material.⁴³ In King et al, the BPE level was found to be a highly significant predictor of breast cancer risk, increasing significantly for women with moderate or marked BPE. Results demonstrated that background parenchymal enhancement has the potential to serve as a tool for risk stratification and may be useful for monitoring chemopreventive strategies.⁴⁴ In Dontchos et al, women with a BPE of mild, moderate, or marked were nine times more likely to develop breast cancer than women with a minimal level of BPE, suggesting that BPE may be able to indicate physiologically active breast tissue, which might lead to malignant transformation⁴⁵ (Fig. 12).

Recently, overall risk assessment models that are image-based are being developed. Portnoi et al recently developed an image-based deep-learning model that utilizes a single 2D maximum intensity projection image from contrast-enhanced to predict the risk of breast cancer in a high-risk patient population. The results showed improved personalized risk assessment for the image-based model compared with the Tyrer Cuzick (v. 8) model.⁷⁷

The growing use of MRI to predict the risk of breast cancer combined with increasing quantitative imaging

biomarkers lends itself to the expansion of AI in breast cancer risk assessment and prediction. Recent studies have shown breast density and parenchymal patterns as well as enhancement to be promising imaging biomarkers that may refine risk assessment models if incorporated. Further augmentation with AI will potentially have important clinical implications in the personalized assessment and screening guideline recommendations for the individual patient.

Conclusion

In a growing era of precision medicine, the "one-size-fits-all" philosophy is no longer clinically relevant. Diagnostic and treatment recommendations are driven by focused quantitative data specific to the patient's genetic, phenotypic, and environmental characteristics.

Breast cancer care continues to evolve with newer imaging techniques, complex treatment protocols, and multidisciplinary management plans. The intricate relationships between these various sectors, combined with the inherent tumor features, lends itself to the growing expansion and integration of radiogenomics in all aspects of clinical decision-making. The detection of suspicious lesions in a multimodality format is possible with the use of newer CADe systems that rely on early-phase kinetics derived from high-temporal resolution MRI techniques. The diagnosis of suspicious lesions continues to be refined, now predicting tumor subtypes and tumor recurrence based on computer-extracted MRI features. The therapeutic response is tailored towards tumor subtype with prognostic information garnered from response of tumor to neoadjuvant therapy. Finally, risk assessment can be predicted from more accurate assessments of fibroglandular tissue and background parenchymal enhancement. The integration of AI in breast imaging may allow for the creation of imaging biomarkers that incorporate patient- and tumor-inherent characteristics and thereby risk-stratify patients with personalized imaging guidelines.

Overall, the role of AI in breast MRI interpretation will continue to evolve, noting that its role will not replace the

radiologist, but rather aid them with new effective and efficient tools. Although clinical reader studies have been done to assess the benefit of computer outputs to radiologists, long-term clinical trials have not yet been conducted.

Disclosures

M.L.G. is a stockholder in R2 Technology/Hologic and a cofounder, equity holder, and scientific advisor in Quantitative Insights/Qlarity Imaging. M.L.G. receives royalties from Hologic, GE Medical Systems, MEDIAN Technologies, Riverain Medical, Mitsubishi, and Toshiba. It is the University of Chicago Conflict of Interest Policy that investigators disclose publicly actual or potential significant financial interest that would reasonably appear to be directly and significantly affected by the research activities.

Acknowledgment

Contract grant sponsor: National Institutes of Health (NIH); Contract grant number: CA195564.

References

1. American Cancer Society website. Cancer facts and figures 2016. <https://www.cancer.org/research/cancer-facts-statistics/all-cancer-facts-figures/cancer-facts-figures-2016.html>
2. National Cancer Institute website. SEER stat fact sheets: Female breast cancer. <https://seer.cancer.gov/statfacts/html/breast.html>
3. Tabar L, Yen MF, Vitak B, Chen HH, Smith RA, Duffy SW. Mammography service screening and mortality in breast cancer patients: 20-year follow-up before and after introduction of screening. *Lancet* 2003;361:1405–1410.
4. Feig S. Cost-effectiveness of mammography, MRI, and ultrasonography for breast cancer screening. *Radiol Clin North Am* 2010;48:879–891.
5. Nelson HD, O'Meara ES, Kerlikowske K, Balch S, Miglioretti D. Factors associated with rates of false-positive and false-negative results from digital mammography screening: An analysis of registry data. *Ann Intern Med* 2016;164:226–235.
6. American College of Radiology website. ACR Appropriateness criteria: Breast cancer screening. <https://acsearch.acr.org/docs/70910/Narrative>. Date of origin 2012. Last review date 2016.
7. Lee CH, Dershaw DD, Kopans D, et al. Breast cancer screening with imaging: Recommendations from the Society of Breast Imaging and the ACR on the use of mammography, breast MRI, breast ultrasound, and other technologies for the detection of clinically occult breast cancer. *J Am Coll Radiol* 2010;7:18–27.
8. Giger ML. Computerized image analysis in breast cancer detection and diagnosis. *Semin Breast Dis* 2002;5:199–210.
9. Giger ML, Chan HP, Boone J. Anniversary paper: History and status of CAD and quantitative image analysis: The role of medical physics and AAPM. *Med Phys* 2008;35:5799–5820.
10. Song SE, Seo BK, Cho KR, et al. Computer aided detection (CAD) system for breast MRI in assessment of local tumor extent, nodal status, and multifocality of invasive breast cancers: Preliminary study. *Cancer Imaging* 2015;15:1.
11. Gillies RJ, Kinahan PE, Hricak H. Radiomics: Images are more than pictures, they are data. *Radiology* 2016;278:563–577.
12. Gubern-Mérida A, Vreemann S, Martí R, et al. Automated detection of breast cancer in false-negative screening MRI studies from women at increased risk. *Eur J Radiol* 2016;85:472–479.
13. Dalmyís MU, Gubern-Merida A, Vreemann S, et al. A computer-aided diagnosis system for breast DCE-MRI at high spatiotemporal resolution. *Med Phys* 2016;43:84–94.
14. Lee CH, Dershaw DD, Kopans D, et al. Breast cancer screening with imaging: Recommendations from the Society of Breast Imaging and the ACR on the use of mammography, breast MRI, breast ultrasound, and other technologies for the detection of clinically occult breast cancer. *J Am Coll Radiol* 2010;7:18–27.
15. Saslow D, Boetes C, Burke W, et al. American Cancer Society guidelines for breast screening with MRI as an adjunct to mammography. *CA Cancer J Clin* 2007;57:75–89.
16. Sheth D, Abe H. Abbreviated MRI and accelerated MRI for screening and diagnosis of breast cancer. *TMRI* 2017;26:183–189.
17. Parmar C, Barry JD, Hosny A, et al. Data analysis strategies in medical imaging. *Clin Cancer Res* 2018;24:3492–3499.
18. Wu J, Sun X, Want J, et al. Identifying relations between imaging phenotypes and molecular subtypes of breast cancer: Model discovery and external validation. *J Magn Reson Imaging* 2017;46:1017–1027.
19. Grimm LJ, Zhang J, Baker JA, Soo MS, Johnson KS, Mazurowski MA. Relationships between MRI Breast Imaging-Reporting and Data System (BI-RADS) lexicon descriptors and breast cancer molecular subtypes: Internal enhancement is associated with luminal B subtype. *Breast J* 2017;23:579–582.
20. Ashraf AB, Daye D, Gavenonis S, et al. Identification of intrinsic imaging phenotypes for breast cancer tumors: Preliminary associations with gene expression profiles. *Radiology* 2014;272:374–384.
21. Li H, Zhu Y, Burnside ES, et al. MR imaging radiomics signatures for predicting the risk of breast cancer recurrence as given by research versions of MammaPrint, Oncotype DX, and PAM50 gene assays. *Radiology* 2016;281:382–391.
22. Platel B, Mus R, Welte T, et al. Automated characterization of breast lesions imaged with an ultrafast DCE-MR protocol. *IEEE Trans Med Imaging* 2013;33:225–232.
23. Wu S, Berg W, Zuley ML, et al. Breast MRI contrast enhancement kinetics of normal parenchyma correlate with presence of breast cancer. *Breast Cancer Res* 2016;18:76.
24. Mariscotti G, Houssami N, Durando M, et al. Accuracy of mammography, digital breast tomosynthesis, ultrasound and MR imaging in pre-operative assessment of breast cancer. *Anticancer Res* 2014;34:1219–1225.
25. Yuan Y, Chen XS, Liu SY, Shen KW. Accuracy of MRI in prediction of pathologic complete remission in breast cancer after preoperative therapy: A meta-analysis. *AJR Am J Roentgenol* 2010;195:260–268.
26. Wu LM, Hu JN, Gu HY, Hua J, Chen J, Xu JR. Can diffusion-weighted MR imaging and contrast-enhanced MR imaging precisely evaluate and predict pathological response to neoadjuvant chemotherapy in patients with breast cancer? *Breast Cancer Res Treat* 2012;135:17–28.
27. Marinovich ML, Houssami N, Macaskill P, et al. Meta-analysis of magnetic resonance imaging in detecting residual breast cancer after neoadjuvant therapy. *J Natl Cancer Inst* 2013;105:321–333.
28. Croshaw R, Shapiro-Wright H, Svensson E, Erb K, Julian T. Accuracy of clinical examination, digital mammogram, ultrasound, and MRI in determining postneoadjuvant pathologic tumor response in operable breast cancer patients. *Ann Surg Oncol* 2011;18:3160–3163.
29. Hylton NM, Blume JD, Berreuter WK, et al. Locally advanced breast cancer: MR imaging for prediction of response to neoadjuvant chemotherapy—Results from ACRIN 6657/I-SPY TRIAL. *Radiology* 2012;263:663–672.
30. Hylton NM, Gatsonis CA, Rosen MA, et al. Neoadjuvant chemotherapy for breast cancer: Functional tumor volume by MR imaging predicts recurrence-free survival—Results from the ACRIN 6657/CALGB 150007 I-SPY 1 TRIAL. *Radiology* 2016;279:44–55.
31. Veer Lvt, Dai H, Vijver M, et al. Gene expression profiling predicts clinical outcome of breast cancer. *Nature* 2002;415:530–536.

32. Prat A, Parker J, Fan C, Perou C. PAM50 assay and the three-gene model for identifying the major and clinically relevant molecular subtypes of breast cancer. *Breast Cancer Res Treat* 2012;135:301–306.
33. Parker J, Mullins M, Cheany M, et al. Supervised risk predictor of breast cancer based on intrinsic subtypes. *J Clin Oncol* 2009;27:1160–1167.
34. Harris LN, Ismail N, McShane LM, et al. Use of biomarkers to guide decisions on adjuvant systemic therapy for women with early-stage invasive breast cancer: American Society of Clinical Oncology Clinical Practice Guideline. *J Clin Oncol* 2016;34:1134–1150.
35. Giger ML, Karssemeijer N, Schnabel JA. Breast image analysis for risk assessment, detection, diagnosis, and treatment of cancer. *Annu Rev Biomed Eng* 2013;15:327–357.
36. Boyd N, Martin L, Yaffe J, Minkin S. Mammographic density and breast cancer risk: Current understanding and future prospects. *Breast Cancer Res* 2011;13:223.
37. Huo Z, Giger ML, Olopade OI, et al. Computerized analysis of digitized mammograms of BRCA1 and BRCA2 gene mutation carriers. *Radiology* 2002;225:519–526.
38. Wei J, Chan HP, Wu YT, et al. Association of computerized mammographic parenchymal pattern measure with breast cancer risk: A pilot case-control study. *Radiology* 2011;260:42–49.
39. Saftlas AF, Hoover RN, Brinton LA, et al. Mammographic densities and risk of breast cancer. *Cancer* 1991;67:2833–2838.
40. Wolfe JN, Saftlas AF, Salane M. Mammographic parenchymal patterns and quantitative evaluation of mammographic densities: A case-control study. *AJR Am J Roentgenol* 1987;148:1087–1092.
41. Byrne C, Schairer C, Wolfe J, et al. Mammographic features and breast cancer risk: Effects with time, age, and menopause status. *J Natl Cancer Inst* 1995;87:1622–1629.
42. Boyd NF, Byng JW, Jong RA, et al. Quantitative classification of mammographic densities and breast cancer risk: Results from the Canadian National Breast Screening Study. *J Natl Cancer Inst* 1995;87:670–675.
43. Morris EA. Diagnostic breast MR imaging: Current status and future directions. *Radiol Clin North Am* 2007;45:863–880, vii.
44. King V, Brooks JD, Bernstein JL, et al. Background parenchymal enhancement at breast MR imaging and breast cancer risk. *Radiology* 2011;260:50–60.
45. Dontchos B, Rahbar H, Partridge S, et al. Are qualitative assessments of background parenchymal enhancement, amount of fibroglandular tissue on MR images and mammographic density associated with breast cancer risk? *Radiology* 2015;276:371–380.
46. Dalmis MU, Vreeman S, Kooi T, et al. Fully automated detection of breast cancer in screening MRI using convolutional neural networks. *J Med Imaging* 2018;5:014502.
47. Giger ML. Machine learning in medical imaging. *J Am Coll Radiol* 2018;15(3 Pt B):512–520.
48. Sahiner B, Pezeshk A, Hadjiiski LM, et al. Deep learning in medical imaging and radiation therapy. *Med Phys* 2018 [Epub ahead of print].
49. Kooi T, Litjens G, van Ginneken B, et al. Large scale deep learning for computer aided detection of mammographic lesions. *Med Image Anal* 2017;35:303–312.
50. Ribli D, Horvath A, Unger Z, Pollner P, Csabai I. Detecting and classifying lesions in mammograms with deep learning. *Sci Rep* 2018;8:4165.
51. Zhang W, Doi K, Giger ML, Wu Y, Nishikawa RM, Schmidt RA. Computerized detection of clustered microcalcifications in digital mammograms using a shift-invariant artificial neural network. *Med Phys* 1994;21:517–524.
52. Chen W, Giger ML, Bick U. A fuzzy c-means (FCM) based approach for computerized segmentation of breast lesions in dynamic contrast-enhanced MR images. *Acad Radiol* 2006;13:63–72.
53. Chen W, Giger ML, Bick U, Newstead G. Automatic identification and classification of characteristic kinetic curves of breast lesions on DCE-MRI. *Med Phys* 2006;33:2878–2887,
54. Chen W, Giger ML, Li H, Bick U, Newstead G. Volumetric texture analysis of breast lesions on contrast-enhanced magnetic resonance images. *Magn Reson Med* 2007;58:562–571.
55. Shimauchi A, Giger ML, Bhoochan N, et al. Evaluation of clinical breast MR imaging performed with prototype computer-aided diagnosis breast MR imaging workstation: Reader study. *Radiology* 2011;258:696–704.
56. Antropova N, Huynh BQ, Giger ML. A deep fusion methodology for breast cancer diagnosis demonstrated on three imaging modality datasets. *Med Phys online* 2017 [Epub ahead of print] <https://doi.org/10.1002/mp.12453>.
57. Antropova N, Abe H, Giger ML. Use of clinical MRI maximum intensity projections for improved breast lesion classification with deep CNNs. *J Med Imaging* 2018;5:014503.
58. Antropova N, Giger ML, Huynh B. Breast lesion classification based on DCE-MRI sequences with long short-term memory networks. *J Med Imaging* 2018;6:011002.
59. Huynh BQ, Li H, Giger ML. Digital mammographic tumor classification using transfer learning from deep convolutional neural networks. *J Med Imaging* 2016;3:034501.
60. Samala RK, Chan HP, Hadjiiski LM, Helvie MA, Richter C, Cha K. Evolutionary pruning of transfer learned deep convolutional neural network for breast cancer diagnosis in digital breast tomosynthesis. *Phys Med Biol* 2018;63:095005.
61. Samala RK, Chan HP, Hadjiiski LM, Helvie MA, Cha KH, Richter CD. Multi-task transfer learning deep convolutional neural network: Application to computer-aided diagnosis of breast cancer on mammograms. *Phys Med Biol* 2017;62:8894–8908.
62. Li H, Giger ML, Huynh BQ, Antropova NO. Deep learning in breast cancer risk assessment: Evaluation of convolutional neural networks on a clinical dataset of full-field digital mammograms. *J Med Imaging* 2017;4:041304.
63. Li H, Zhu Y, Burnside ES, Perou CM, Ji Y, Giger ML. Quantitative MRI radiomics in the prediction of molecular classifications of breast cancer subtypes in the TCGA/TCIA dataset. *Breast Cancer* 2016;2:16012.
64. Drukker K, Li H, Antropova N, Edwards A, Papaioannou J, Giger ML. Most-enhancing tumor volume by MRI radiomics predicts recurrence-free survival "early on" in neoadjuvant treatment of breast cancer. *Cancer Imaging* 2018;18:12.
65. Mohamed AA, Berg WA, Peng H, Luo Y, Jankowitz RC, Wu S. A deep learning method for classifying mammographic breast density categories. *Med Phys* 2018;45:314–321.
66. Sutton EJ, Huang EP, Drukker K. Breast MRI radiomics: Comparison of computer- and human-extracted imaging phenotypes. *Eur Radiol Exp* 2017;1(22).
67. Zhu Y, Li H, Guo W, et al. Deciphering genomic underpinnings of quantitative MRI-based radiomic phenotypes of invasive breast carcinoma. *Sci Rep* 2015;5:17787.
68. Gubern-Merida A, Marti R, Melendz J, et al. Automated localization of breast cancer in DCE-MRI. *Med Image Anal* 2015;20:265–274.
69. Chang Y-C, Huang Y-H, Huang C-S, Chen J-H, Chang R-F. Computerized breast lesion detection using kinetic and morphologic analysis for dynamic contrast-enhanced MRI. *Magn Reson Imaging* 2014;32:514–522.
70. Chang Y-C, Huang Y-H, Huang C-S, Change P-K, Chen J-H, Chang R-F. Classification of breast mass lesions using model-based analysis of the characteristic kinetic curve derived from fuzzy c-means clustering. *Magn Reson Imaging* 2012;30:312–322.
71. Fowler AM, Mankoff DA, Joe BN. Imaging neoadjuvant therapy response in breast cancer. *Radiology* 2017;285:358–375.
72. Pan J, Dogann BE, Carkaci S, et al. Comparing performance of the CAD stream and the DynaCAD breast MRI CAD systems. *J Digit Imaging* 2013;26:971–976.
73. Freer P. Mammographic breast density: Impact on breast cancer risk and implications for screening. *Radiographics* 2015;35:302–315.

74. Dalmis Mu, Litjens G, Holland K, et al. Using deep learning to segment breast and fibroglandular tissue in MRI volumes. *Med Phys* 2017;44:533–546.
75. Brentnall AR, Cuzick J, Buist DS, Bowles EJA. Long-term accuracy of breast cancer risk assessment combining classic risk factors and breast density. *JAMA Oncol* 2018;4:e180174.
76. Warwick J, Birke H, Stone J, et al. Mammographic breast density refines Tyrer-Cuzick estimates of breast cancer risk in high-risk women. *Breast Cancer Res* 2014;16:451.
77. Portnoi T, Yala A, Schuster T, et al. Deep learning model to assess cancer risk on the basis of a breast MR image alone. *Am J Radiol* 2019;213:227–233.
78. Meinel LA, Stolpen AH, Berbaum KS, Fajardo LL, Reinhardt JM. Breast MRI lesion classification: Improved performance of human readers with a backpropagation neural network computer-aided diagnosis (CAD) system. *J Magn Reson Imaging* 2007;25:89–95.
79. Ravichandran K, Braman N, Janowczyk A, Madabhushi A. A deep learning classifier for prediction of pathological complete response to neoadjuvant chemotherapy from baseline breast DCE-MRI. In: Proc SPIE 10575, Medical Imaging 2018: Computer-Aided Diagnosis 105750C 2018 [Epub ahead of print] doi:<https://doi.org/10.1117/12.2294056>.
80. Nishikawa RM, Doi K, Giger ML, et al. Computerized detection of clustered microcalcifications: Evaluation of performance using mammograms from multiple centers. *RadioGraphics* 1995;15:443–452.
81. Gilhuijs KGA, Giger ML, Bick U. Automated analysis of breast lesions in three dimensions using dynamic magnetic resonance imaging. *Med Phys* 1998;25:1647–1654.
82. Sahiner B, Pezeshk A, Hadjiiski LM, et al. Deep learning in medical imaging and radiation therapy. *Med Phys* 2019;46:e1–e36.
83. Bi WL, Hosny A, Schabath MB, et al. Artificial intelligence in cancer imaging: Clinical challenges and applications. *CA Cancer J Clin* 2019;69:127–157.